Kobe University Repository : Kernel

PDF issue: 2025-12-05

Below bulk-band-gap photoluminescence at room temperature from heavily P- and B-doped Si nanocrystals

Fujii, Minoru
Toshikiyo, Kimiaki
Takase, Yuji
Yamaguchi, Yasuhiro
Hayashi, Shinji

(Citation)
Journal of Applied Physics,94(3):1990-1995

(Issue Date)
2003-08

(Resource Type)
journal article

(Version)
Version of Record

(URL)
https://hdl.handle.net/20.500.14094/90000280

KOBE UNIVERSITY

Below bulk-band-gap photoluminescence at room temperature from heavily P- and B-doped Si nanocrystals

Minoru Fujii,[a] Kimiaki Toshikiyo, Yuji Takase, Yasuhiro Yamaguchi, and Shinji Hayashi
Department of Electrical and Electronics Engineering, Faculty of Engineering, Kobe University, Rokkodai, Nada, Kobe 657-8501, Japan

(Received 1 April 2003; accepted 19 May 2003)

Photoluminescence (PL) properties of heavily P- and B-doped Si nanocrystals (nc-Si) are studied. By simultaneously doping two types of impurities, nc-Si exhibit strong PL at around 0.9 eV at room temperature. The temperature quenching of the PL is very small. Although the PL peak energy is very close to that of dangling-bond related PL previously observed, all of the observed properties, i.e., decay dynamics, degree of temperature quenching, etc., are apparently different. The transition between donor and acceptor states in nc-Si is the possible origin of the low-energy PL. © *2003 American Institute of Physics.* [DOI: 10.1063/1.1590409]

I. INTRODUCTION

It is well known that luminescence energy of Si nanocrystals (nc-Si) can be tuned from a bulk bandgap (1.12 eV) to the visible region by simply controlling the size.[1,2] The temperature quenching of this luminescence is very small and it is observed at room temperature. Based on detailed optical studies, these near infrared to red luminescence are assigned to the recombination of excitons confined in nc-Si.[1–6]

In addition to the exciton luminescence, broad luminescence has been observed at around 0.8 to 1.0 eV for some kinds of nc-Si systems.[2,7–9] Dangling bond defects at Si/SiO_2 interfaces are considered to be responsible for this luminescence. The luminescence energy can also be tuned by the size of nc-Si, although the size dependent shift is about half that of the exciton luminescence.[2,8,9] This luminescence shows strong temperature quenching, and luminescence intensity at room temperature is extremely weak. If efficient luminescence is realized below the band gap of bulk Si crystals at room temperature, application of nc-Si will be extended to the field of optical telecommunications, because silica-based fiber telecommunication utilizes light in the wavelength range of 1.3 to 1.6 μm.

One approach to realize room-temperature below bulk-band-gap luminescence from nc-Si is to introduce luminescing species in nc-Si assemblies and indirectly excite the species by the energy transfer from nc-Si. The most important example of this approach is Er doping. It has been demonstrated that if Er^{3+} is in the vicinity of nc-Si, it is excited very efficiently by the energy transfer from nc-Si, and exhibits strong photoluminescence (PL) at 0.81 eV at room temperature.[10–13] Based on this approach, planer-waveguide-type optical amplifiers and electroluminescence devices have been realized.[14,15]

In this article, we report another approach to realize room-temperature below bulk-band-gap PL from nc-Si. This approach does not use luminescing species like Er^{3+}, but controls the electronic band structure of nc-Si by shallow impurity doping.

Doping of shallow impurities causes the formation of impurity states in the band gap of nc-Si. The transition of electrons between the states and a conduction (valence) band may exhibit PL below the energy of exciton PL of nc-Si. However, since the conduction- (valence-) band edge is shifted to higher (lower) energy by the quantum size effects, the transition energy is expected to be larger than the band-gap energy of bulk Si crystals. In order to realize below bulk-band-gap PL, we dope *n*- and *p*-type impurities simultaneously into nc-Si. In this system, electronic transition between donor and acceptor states is possible. Since the energy levels of hydrogenic impurities are not strongly affected by the size of the nc-Si,[16,17] the transition between the states will be below the bulk Si band-gap even if the size of the host Si is in the range of nanometers.

II. EXPERIMENTAL PROCEDURE

P- and B-doped nc-Si were prepared by a cosputtering method.[18–23] Si, borosilicate glass (BSG), and phosphosilicate glass (PSG) were simultaneously sputterdeposited in Ar gas, and the deposited films (about 1 μm in thickness) were annealed in a N_2 gas (99.999%) atmosphere for 30 min at 1150 °C. nc-Si were grown in borophosphosilicate glass (BPSG) films during the annealing. P (B) concentration in films was controlled by changing the P_2O_5 (B_2O_3) concentration in the PSG (BSG) sputtering targets. The average concentration of P_2O_5 in a whole film (C_P) was determined by an electron probe microanalysis, and that of B_2O_3 (C_B) by the intensity ratio of Si–O and B–O vibration signals in infrared absorption spectroscopy.[24] In this method, the size of nc-Si can be controlled by changing the concentration of Si in films or the annealing temperature. The average size of nc-Si was estimated by cross-sectional transmission electron microscopic (TEM) observations.

Figure 1 shows a TEM image of a sample with high P and B concentration ($C_P = 1.26$ mol % and $C_B = 1.25$ mol %).

[a]Author to whom correspondence should be addressed; electronic mail: fujii@eedept.kobe-u.ac.jp

 © 2003 American Institute of Physics

Downloaded 13 Jul 2007 to 133.30.51.109. Redistribution subject to AIP license or copyright, see http://jap.aip.org/jap/copyright.jsp

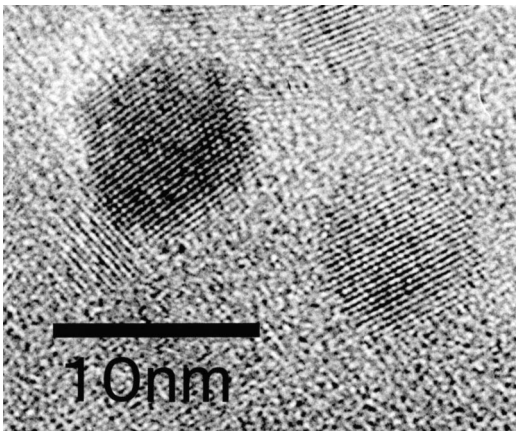

FIG. 1. TEM image of nc-Si in a BPSG thin film. Lattice fringes corresponding to {111} plans of Si can clearly be seen. Nanocrystals are almost spherical and crystallinity is very good.

Nanocrystals are almost spherical and lattice fringes corresponding to {111} planes of Si are clearly seen in Fig. 1. TEM observations revealed that at low P and B concentrations the size of nc-Si is almost independent of impurity concentration, while at high concentration (e.g., >1 mol %), the average size becomes larger than that of nc-Si in pure SiO_2 with the same Si concentration. Furthermore, size distribution becomes broader with increasing impurity concentration. Especially, a gradient of the size appears on the direction of the sample depth; the average size near a substrate is larger than that near a surface. The softening of matrices by P and B doping and the resulting longer diffusion length of Si atoms during annealing makes particles larger. This also makes size distribution broader because Si atoms that diffuse to the surface of films are oxidized by residual oxygen in an annealing atmosphere. The largest average diameter of nc-Si studied in this work was about 10 nm.

The evidence that impurities are doped into substitutional sites of nc-Si and are electrically active is obtained from infrared absorption measurements. If either P or B is doped, broad absorption which continuously increases to a longer-wavelength region appears and this absorption becomes stronger with increasing impurity concentration.[18] This absorption is assigned to the intraconduction- (intravalence) band transition of carriers supplied by impurity doping. We have studied infrared absorption spectra as a function of P and B concentration. We found that under a fixed B (P) concentration, the increase of P (B) concentration results in the quenching of this absorption. This means that carriers are compensated in nc-Si. It is worth noting that in nc-Si, the number of impurities is very small even if the impurity concentration is very high, and thus it is changed digitally. Therefore, if the average number of P and B in a whole system is nearly the same, it is possible that, in some particles in a sample, the numbers of donors and acceptors are exactly the same; there exists some perfectly compensated nc-Si.

Unfortunately, the number of active dopants or excess carriers in nanocrystals cannot simply be estimated from average P or B concentrations because of the following reasons. First, it is not clear whether dopants are uniformly distributed in samples or segregated in some regions, e.g., at interfaces between nanocrystals and matrices. The distribution may also depend on the kind of impurities. Second, the number of excess carriers is not always the same as that of dopants. It may depend on the size and quality, i.e., the number of defects, of nc-Si. Third, since size distribution exists in samples, statistically, doping starts from larger nc-Si in size distribution and proceeds to smaller ones with increasing dopant concentration.

However, rough estimation is possible. In our previous work on electron spin resonance of P-doped samples,[21] with increasing P concentration, defect-related signals became weaker and a hyperfine structure of conduction electron signal emerged. For example, with $C_P=0.4$ mol % and an average nc-Si diameter of 5.8 nm, both defect-related and conduction–electron related signals were observed. If we assume that nc-Si with the average diameter has one electrically active P and smaller ones are still pure, the average P concentration in nc-Si with the average size is $\sim 1 \times 10^{19}$ cm^{-3}. In the same study, at $C_P=1.2$ mol %, both the defect-related and hyperfine structure of conduction electron signals disappeared, and only the broad conduction electron signal remained. This suggests that in majority of nc-Si in size distribution, more than two electrically active P exist, corresponding to the dopant concentration of $\sim 10^{20}$ cm^{-3}.

Since we cannot estimate the exact number of active dopants in nanocrystals, we also cannot know the number of compensated nc-Si in the samples. Therefore, in this work, we fixed the B concentration to some values and changed only the P concentration. With this approach, we can find an optimum condition to maximize the number of compensated nc-Si from the PL intensity, because the PL intensity of a compensated nc-Si is expected to be larger than that of an uncompensated nc-Si.

PL spectra were measured using a single monochromator equipped with an InP/InGaAs photocathode near-infrared photomultiplier. The excitation source was the 488 nm line of an Ar-ion laser. The excitation power was 4 mW/cm^2. The laser beam was chopped by using an acousto-optic modulator at a frequency of 16 Hz. The spectral response of the detection system was calibrated with the aid of a reference spectrum of a standard tungsten lamp. The PL decay curves were measured by pumping to steady state and chopping the laser with the same frequency as used for the PL measurements. The overall time resolution of the system was about 40 ns. The PL and the PL decay dynamics were measured from 4 to 295 K in a continuous-flow He cryostat.

III. RESULTS AND DISCUSSION

A. B doping

Before doping P and B simultaneously in nc-Si, we summarize how the PL spectra of nc-Si is modified by B doping.[19,20] Figure 2 shows PL spectra of pure and B-doped nc-Si at room temperature. Pure nc-Si exhibits a broad PL peak centered at around 1.35 eV. The PL is assigned to the recombination of excitons confined in nc-Si. By doping B, the spectrum is strongly modified. First, the intensity is decreased significantly. Second, a long tail appears on the low-

Downloaded 13 Jul 2007 to 133.30.51.109. Redistribution subject to AIP license or copyright, see http://jap.aip.org/jap/copyright.jsp

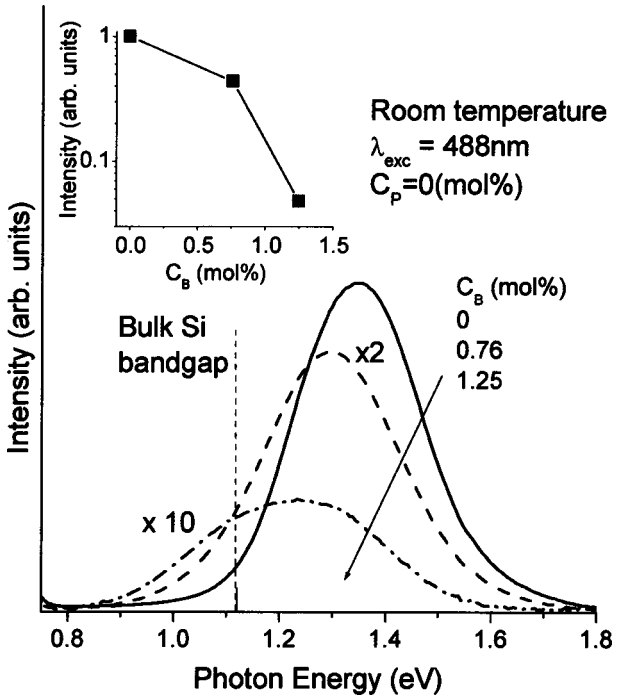

FIG. 2. PL spectra of B-doped Si nanocrystals. For better comparison of spectral shape, the spectra of B-doped samples are scaled by the indicated multiplication factor. With increasing B concentration, PL becomes weaker and a broad tail appears below the band gap of bulk Si crystals. The integral intensity of the spectra are plotted in the inset.

energy side, and the tail penetrates below the band gap of bulk Si crystals. In the inset of Fig. 2, the integral PL intensity is plotted as a function of B concentration. The intensity is decreased down to 5% of the value of pure nc-Si at the highest B concentration. The observed quenching is considered to be due to the small PL quantum efficiency of B-doped nc-Si because nonradiative Auger recombination of excitons with the interaction of holes supplied by B doping is very efficient.[19,20] However, this does not always mean that PL observed in B-doped samples comes only from pure nc-Si remaining undoped in samples. The fact that the PL tail penetrates into below the bulk Si band gap indicates that at least the low-energy tail part of the spectra arises from B-doped nc-Si.

In Fig. 2, the PL peak shifts to lower energy with increasing B concentration. However, this does not always happen. We have studied more than five series of similar samples. Although the quenching and broadening of PL were observed for all the samples, the low energy shift was not reproduced in some samples. In the case of pure nc-Si, our preparation method is very stable, and PL peak energy is controlled with good accuracy; only for heavily impurity-doped samples, the PL properties fluctuated. As just described, there exists large inhomogeneity in heavily impurity-doped samples. This inhomogeneity is considered to be responsible for the observed fluctuation of PL properties.

B. B and P doping

Now, we dope P and B simultaneously and see how the PL spectrum is developed with increasing P concentration.

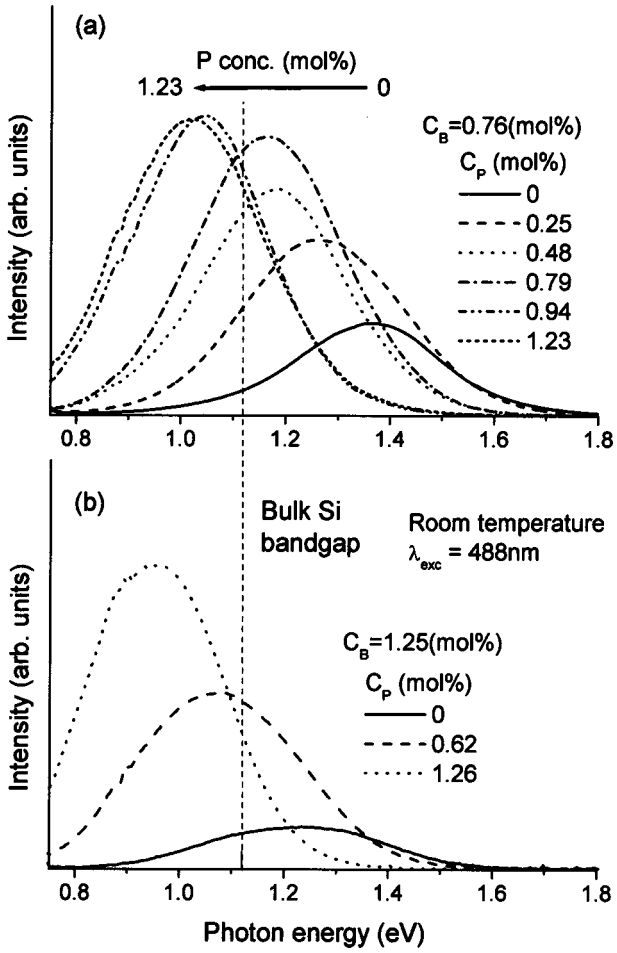

FIG. 3. P concentration dependence of PL spectra. B concentration is fixed to (a) $C_B = 0.76$ mol % and (b) $C_B = 1.25$ mol %, and P concentration is increased up to 1.26 mol %.

Figure 3 shows PL spectra of P- and B-doped nc-Si. In Fig. 3(a), C_B is fixed to 0.76 mol % and C_P is changed from 0 to 1.23 mol %. In Fig. 3(b), C_B is fixed to 1.25 mol % and C_P is changed from 0 to 1.26 mol %. In both cases, the PL shows similar behavior. PL peak shifts continuously to a lower energy, crosses the band gap of bulk Si crystals and reaches around 0.95 eV (Fig. 4). The other important effect of P doping is the enhancement of the PL intensity. In Fig. 3(b), the PL intensity is increased more than five times by P doping, meaning that quenching of PL by B doping is largely recovered by adding P; the PL intensity of the sample with $C_B = 1.25$ mol % and $C_P = 1.26$ mol % is about 30% of that of pure nc-Si.

However, here we also have a problem of reproducibility. The increase in PL intensity was observed for all series of samples until $C_P \simeq 0.9\%$. On the other hand, above that concentration, intensity was not always increased, and sometimes it was decreased. This fluctuation of the PL intensity at a high impurity concentration range may also arise from the inhomogeneity of samples.

Although there still remain difficulties in precisely controlling all sample preparation parameters, the concept of the present approach is very important in view of future photonic application of nc-Si, i.e., the simultaneous doping of P and B

Downloaded 13 Jul 2007 to 133.30.51.109. Redistribution subject to AIP license or copyright, see http://jap.aip.org/jap/copyright.jsp

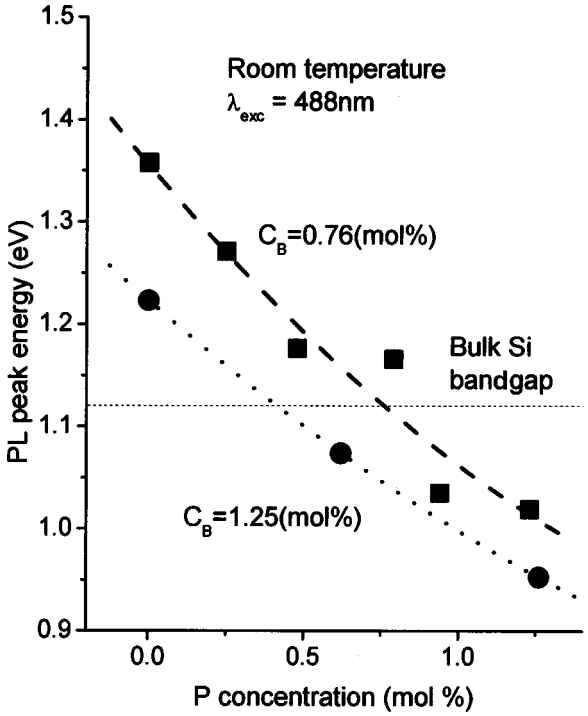

FIG. 4. PL peak energies of P and B codoped nc-Si are plotted as a function of P concentration. B concentration is fixed to 0.76 and 1.25 mol %.

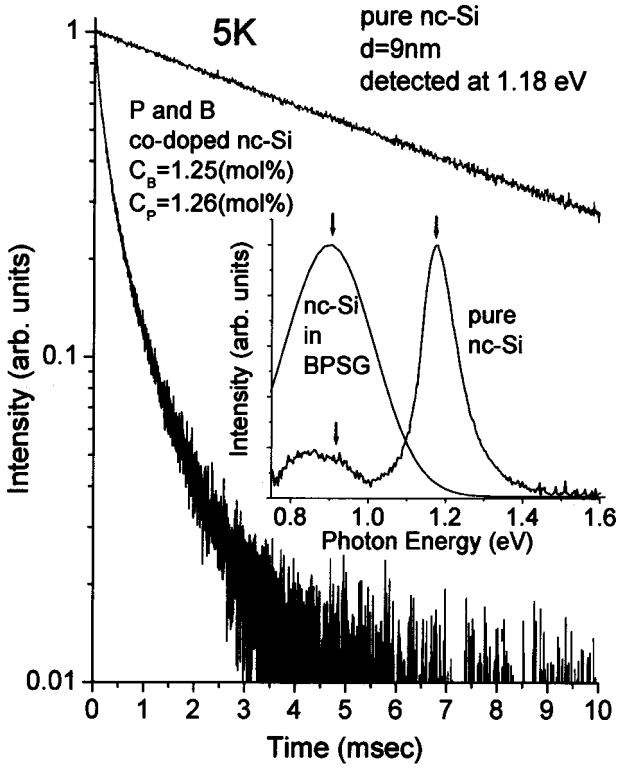

FIG. 5. PL decay curves of P and B codoped nc-Si, and pure nc-Si at 5 K. In the inset, energy positions detecting PL decay curves are indicated by arrows.

in nc-Si offers an opportunity to extend the tunability of PL energy of nc-Si systems below bulk Si band gap without losing its intensity very much.

C. Properties of the low-energy photoluminescence

Figure 5 shows PL decay curves of pure nc-Si, and P and B codoped nc-Si at 5 K. The energy where the PL signal is detected is indicated by arrows in the inset of Fig. 5 (1.18 and 0.92 eV, respectively). The exciton PL of pure nc-Si shows a single-exponential decaying behavior. The lifetime is about 8 ms. On the other hand, the decay curve of codoped nc-Si is far from the single-exponential function and the lifetime is much shorter than the exciton PL of pure nc-Si. We measured the PL lifetime at other energies on broad PL bands. The lifetime was in the range of 100 to 500 μs. Figure 6 shows the temperature dependence of PL lifetime of a codoped sample. The lifetime becomes shorter with increasing temperature. The shortening may be due to an increase of nonradiative recombination processes. In comparison, we measured the decay curve of dangling bond PL of pure nc-Si that is commonly observed for some kinds of nc-Si systems at around 0.9 eV;[2,7–9] the PL detection energy (0.92 eV) is indicated by an arrow in the inset of Fig. 5. The PL lifetime was of the order of μs and much shorter than that of codoped samples, although detecting energy is the same.

In Fig. 7, PL peak intensities of the co-doped nc-Si (■) and nc-Si in pure SiO_2 (average diameter of about 9 nm) (▲) are plotted as a function of temperature. The exciton PL of pure nc-Si shows almost no temperature quenching. The temperature quenching of PL is also very small for codoped samples; the PL intensity at room temperature is about the half of that at 5 K. This small temperature quenching is completely different from that of dangling-bond-related PL. The open triangles in Fig. 7 represent the PL intensity of the dangling-bond-related PL at 0.92 eV. We can see that the PL intensity drops very rapidly with increasing temperature and

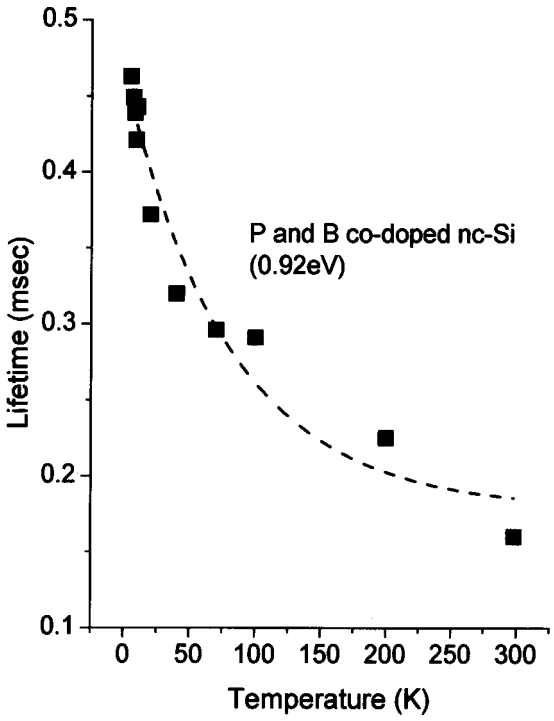

FIG. 6. Temperature dependence of PL lifetime for P and B codoped nc-Si

Downloaded 13 Jul 2007 to 133.30.51.109. Redistribution subject to AIP license or copyright, see http://jap.aip.org/jap/copyright.jsp

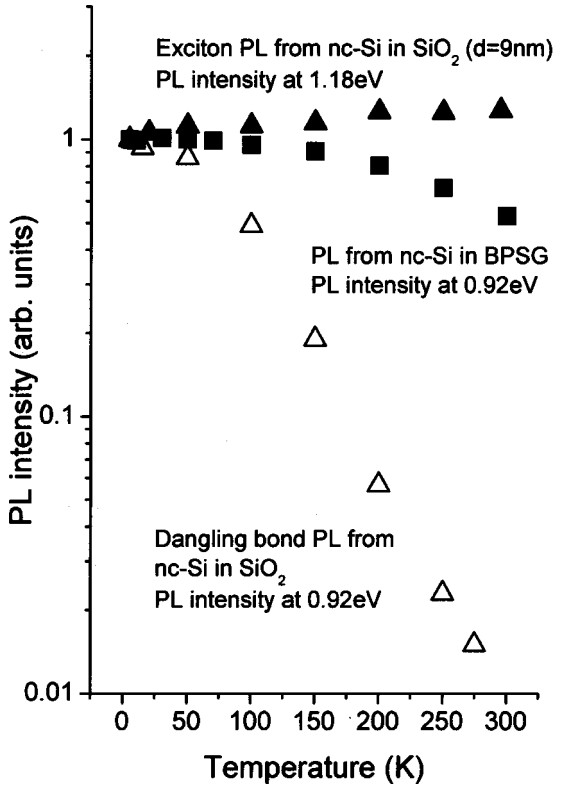

FIG. 7. Temperature dependence of PL peak intensities for nc-Si in BPSG (■) and exciton PL of nc-Si in pure SiO_2 (▲). Intensity of dangling-bond-related PL (△) is also plotted.

that at room temperature is about 1% of that at low temperatures. Figure 7 clearly demonstrates that the mechanism of the low-energy PL is different from that of dangling-bond-related PL previously observed.

The fact that below bulk-band-gap PL was observed only for codoped samples indicates that both donor and acceptor states are involved in the recombination process. PL originating from the transition between the conduction-band tail (donor band) to the valence-band tail (acceptor band) has been observed for heavily doped, compensated bulk Si:P,B.[25] In these systems, as the total number of donor and acceptor impurities increases, PL bands shift to lower energy and are significantly broadened.[25] The mechanism of the low-energy PL observed in this work is considered to be essentially the same as that observed for heavily doped compensated bulk Si:P,B; PL arises from the electronic transition between the conduction- and valence-band tails induced by impurity doping. However, there are some crucial differences. The largest difference appears on the temperature dependence of the PL intensity. In heavily impurity-doped bulk Si crystals, PL is observed only at very low temperatures because excited electrons and holes are easily thermalized or migrated in impurity bands and recombine nonradiatively. On the other hand, in nc-Si, transportation of carriers is limited only within nc-Si. If the surface of nc-Si is perfectly passivated and two types of impurities are compensated, nonradiative recombination processes would be very small. This may result in the observed strong PL and very small temperature quenching. Enhancement of the ionization energy of impurities due to the quantum confinement effect may play a positive role.[21] Furthermore, softening of matrices by introducing P and B heavily in SiO_2 is considered to be partially responsible for the enhancement of PL intensity. Since BPSG is softer than pure nc-Si, stress at nc-Si / matrix interfaces is smaller, resulting in a smaller defect density. This causes a smaller number of defective (dark) nc-Si, and larger number of optically active nc-Si. The observed wide spectral width could be inhomogeneous broadening caused by the distribution of the size and the impurity concentration.

IV. CONCLUSION

In conclusion, we have observed strong room-temperature PL from nc-Si in BPSG thin films at around 0.9 eV. The properties of the low-energy PL were apparently different from those of exciton PL and dangling-bond-related PL. Since the below bulk Si band-gap PL was observed only for P and B codoped nc-Si, the PL was assigned to be due to the electron transition between the donor and acceptor states in nc-Si. With this approach, the luminescence peak energy of nc-Si can be tuned from 0.9 eV to 2.0 eV by controlling the size and the impurity concentrations.

ACKNOWLEDGMENTS

This work was supported by a Grant-in-Aid for Scientific Research from the Ministry of Education, Culture, Sports, Science, and Technology, Japan, and in part by an Industrial Technology Research Grant Program in '02 from New Energy and Industrial Technology Development Organization (NEDO), Japan.

[1] D. Kovalev, H. Heckler, G. Polisski, and F. Koch, Phys. Status Solidi B **215**, 871 (1999).
[2] S. Takeoka, M. Fujii, and S. Hayashi, Phys. Rev. B **62**, 16820 (2000).
[3] M. V. Wolkin, J. Jorne, P. M. Fauchet, G. Allan, and C. Delerue, Phys. Rev. Lett. **82**, 197 (1999).
[4] P. D. J. Calcott, K. J. Nash, L. T. Canham, M. J. Kane, and D. Brumhead, J. Phys.: Condens. Matter **5**, L91 (1993).
[5] J. Diener, D. Kovalev, H. Heckler, G. Polisski, and F. Koch, Phys. Rev. B **63**, 073302 (2001).
[6] D. Kovalev, H. Heckler, B. Averboukh, M. Ben-Chorin, M. Schwartzkopff, and F. Koch, Phys. Rev. B **57**, 3741 (1998).
[7] Y. Mochizuki, M. Mizuta, Y. Ochiai, S. Matsui, and N. Ohkubo, Phys. Rev. B **46**, 12353 (1992).
[8] B. K. Meyer, D. M. Hofmann, W. Stadler, V. Petrova-Koch, F. Koch, P. Omiling, and P. Emanuelsson, Appl. Phys. Lett. **63**, 2120 (1993).
[9] B. K. Meyer, D. M. Hofmann, W. Stadler, V. Petrova-Koch, F. Koch, P. Emanuelsson, and P. Omling, J. Lumin. **57**, 137 (1993).
[10] M. Fujii, M. Yoshida, Y. Kanzawa, S. Hayashi, and K. Yamamoto, Appl. Phys. Lett. **71**, 1198 (1997).
[11] M. Fujii, M. Yoshida, S. Hayashi, and K. Yamamoto, J. Appl. Phys. **84**, 4525 (1998).
[12] P. G. Kik and A. Polman, J. Appl. Phys. **88**, 1992 (2000).
[13] F. Priolo, G. Franzo, D. Pacifici, V. Vinciguerra, F. Iacona, and A. Irrera, J. Appl. Phys. **89**, 264 (2001).
[14] H. Han, S. Seo, and J. H. Shin, Appl. Phys. Lett. **79**, 4568 (2001).
[15] F. Iacona, D. Pacifici, A. Irrera, M. Miritello, G. Franzò, F. Priolo, D. Sanfilippo, G. Di Stefano, and P. G. Fallica, Appl. Phys. Lett. **81**, 3242 (2002).
[16] C. Delerue, M. Lannoo, G. Allan, and E. Martin, Thin Solid Films **255**, 27 (1995).
[17] G. Allan, C. Delerue, M. Lannoo, and E. Martin, Phys. Rev. B **52**, 11982 (1995).

Downloaded 13 Jul 2007 to 133.30.51.109. Redistribution subject to AIP license or copyright, see http://jap.aip.org/jap/copyright.jsp

[18] A. Mimura, M. Fujii, S. Hayashi, D. Kovalev, and F. Koch, Phys. Rev. B **62**, 12625 (2000).
[19] M. Fujii, S. Hayashi, and K. Yamamoto, J. Appl. Phys. **83**, 7953 (1998).
[20] A. Mimura, M. Fujii, S. Hayashi, and K. Yamamoto, Solid State Commun. **109**, 561 (1999).
[21] M. Fujii, A. Mimura, S. Hayashi, Y. Yamamoto, and K. Murakami, Phys. Rev. Lett. **89**, 206805 (2002).
[22] M. Fujii, A. Mimura, S. Hayashi, and K. Yamamoto, Appl. Phys. Lett. **75**, 184 (1999).
[23] M. Fujii, A. Mimura, S. Hayashi, K. Yamamoto, C. Urakawa, and H. Ohta, J. Appl. Phys. **87**, 1855 (2000).
[24] A. S. Tenny, J. Electrochem. Soc. **118**, 1658 (1971).
[25] M. Levy, P. Y. Yu, Y. Zhand, and M. P. Sarachik, Phys. Rev. B **49**, 1677 (1994).

Downloaded 13 Jul 2007 to 133.30.51.109. Redistribution subject to AIP license or copyright, see http://jap.aip.org/jap/copyright.jsp